This is an open access article published under an ACS AuthorChoice License, which permits copying and redistribution of the article or any adaptations for non-commercial purposes.

ORGANOMETALLICS

Article

pubs.acs.org/Organometallics

Metallacyclobutanes from Schrock-Type d^0 Metal Alkylidene Catalysts: Structural Preferences and Consequences in Alkene Metathesis

Xavier Solans-Monfort,*[,†] Christophe Copéret,*[,‡] and Odile Eisenstein*[,§]

[†]Departament de Química, Universitat Autònoma de Barcelona, 08193 Bellaterra, Spain

[‡]Department of Chemistry and Applied Biosciences, ETH Zürich, Vladimir Prelog Weg 1-5, CH-8093 Zürich, Switzerland

[§]Institut Charles Gerhardt, CNRS 5253 Université de Montpellier, cc 1501, Place E. Bataillon, F-34095 Montpellier, France

Supporting Information

ABSTRACT: Metallacyclobutanes have been observed as intermediates in the alkene metathesis reaction, with the 5-coordinated metal center, in a trigonal bipyramidal or a square-planar coordination. Previous calculations have shown that only the trigonal bipyramidal form is directly on the reaction pathway of alkene metathesis. The square-pyramidal form, which is obtained by a trigonal-bipyramidal (TBP)-square-based pyramidal (SP) interconversion at the metal, is an intermediate that can be responsible for catalyst deactivation. This computational study aimed at establishing the factors that control the properties of the two metallacyclobutanes (structural and ^{13}C NMR features, stability, and TBP-SP interconversion) that can influence the efficiency of the metathesis reaction. Metallacyclobutanes resulting from the addition of ethene to a large set of methylidene complexes where the metal fragment is M(E)(X)(Y) (M = Mo or W; E = alkyl imido, aryl imido, or oxo), (X and Y) = alkyl, pyrrolyl, alkoxy and fluoroalkoxy, and large monoaryloxy) have been studied by density functional calculations (B3PW91, and M06). From the study of these numerous complexes that include in particular all characterized complexes, properties of the metallacyclobutanes could be derived: Metallacyclobutanes with W are more stable than those with Mo relative to reactants; electron withdrawing ligands stabilize the two isomeric forms of the metallacyclobutane but more the TBP than the SP form, and conversely, electron donating ligands destabilize both forms but more the TBP isomer. The energy barrier for the TBP-SP interconversion is found to be lower than that for the productive ethene metathesis pathway for W complexes but is generally higher for Mo species. These facts rationalize the experimental evidence and accounts in particular for the high efficiency of the Mo catalysts.

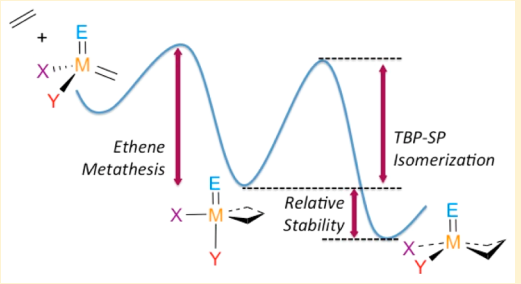

INTRODUCTION

In his original article, Chauvin proposed that the essential intermediates in alkene metathesis were metallacyclobutanes, formed via a [2 + 2] cycloaddition between a metal alkylidene complex and an alkene.[1,2] The reverse step, cycloreversion, generates a new alkylidene complex and an alkene (or eventually the same species in a degenerate metathesis process), which allows trans-alkylidenation and overall alkene metathesis to take place. This mechanism is now well-accepted for all catalysts, namely, d^0 Mo, W, and Re Schrock-type complexes,[3−7] d^6 Ru Grubbs-type catalysts,[8−10] and for ill-defined systems.[11] Computational studies have shown that the metallacyclobutanes on the reaction path for alkene metathesis have a 5-coordinated trigonal-bipyramidal (TBP) coordination at the metal center with the two metal−carbon bonds of the metallacyclobutane occupying two equatorial sites of the TBP.[12−22] However, the square-based pyramidal (SP) isomer is also a minimum on the potential energy surface. In the case of Schrock-type catalysts, calculations on selected representative examples have shown that the SP metallacyclobutanes can be more stable than the corresponding TBP isomers. In this case, the SP metallacyclobutane is thought to be a resting state of the catalyst since the TBP-SP exchange through a turnstile rotation is considered to be easier than cycloreversion, i.e., associated with a lower energy barrier (Scheme 1). Furthermore, the SP metallacyclobutane can also be a possible source for deactivation.[14,15,23] For Grubbs-type catalysts, calculations have shown that TBP are always much more stable than SP isomers; the latter have in fact never been observed and have been calculated to be much higher in energy than the separated reactants (alkylidene complex and alkene).[20,21,24,25] Since both metallacyclobutanes are accessible intermediates in metathesis reactions for d^0 metal, it is thus of major interest to understand the factors that control the structures, the relative stability, and the TBP-SP interconversion process and ultimately to better know how this ensemble of properties influences the alkene metathesis process.

The structural features of the TBP- or SP-metallacyclobutanes, hereafter referred to as **M-TBP** and **M-SP**, respectively,

Received: February 21, 2015
Published: April 27, 2015

 © 2015 American Chemical Society

DOI: 10.1021/acs.organomet.5b00147
Organometallics 2015, 34, 1668−1680

Scheme 1. Metathesis Pathway for the Reaction of Ethene with d^0-[M(E)(=CH_2)(X)(Y)] with Formation of Trigonal-Pyramidal (M-TBP) and Square-Based Pyramidal (M-SP) Metallacyclobutane

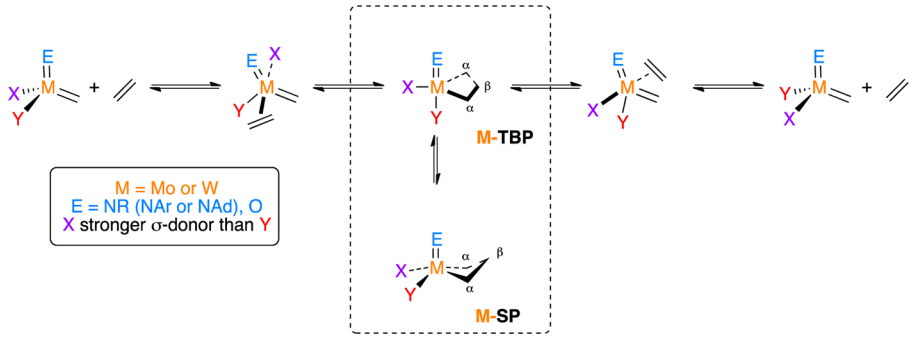

have been determined by solution and solid-state NMR, X-ray diffraction analysis, and computations.[26−38] In NMR, **M-TBP** and **M-SP** have distinctive signatures for the α- and β-carbons. The chemical shifts (δ) of the α-carbons appear between 80 and 110 ppm, while these of the β-carbon range from −5 to 10 ppm in **M-TBP**. In contrast, for **M-SP** the chemical shifts of the α- and β-carbons are similar and around 25−50 ppm, close to those of sp^3-hybridized carbons. Metallacyclobutanes have been characterized by X-ray crystallography, usually for tungsten complexes.[3−5,27,31,32,35,37,38] **M-TBP** and **M-SP** differ by the coordination at the metal center (E, X, and Y are in a *mer* arrangement in TBP and *fac* in SP) and also the shape of the 4-membered ring. Regardless of the nature of the E, X, and Y ancillary ligands, the metallacyclobutane is planar in **M-TBP** with a relatively short M···C_β distance and a C_α-C_β-C_α' angle significantly larger than 109°. In contrast, for **M-SP**, the metallacyclobutane ring is folded with a long M···C_β distance and an angle C_α-C_β-$C_{\alpha'}$ of less than 109°.

Examination of the experimental data on metallacyclobutanes of the general formula M(E)(C_3H_6)(X)(Y) highlights how the electron donating/withdrawing properties of the ligands and their size influence the preference for one of the two structures. Increasing the electron withdrawing ability of either X or Y stabilizes **M-TBP** as shown by the increasing preference of **M-TBP** over **M-SP** upon fluorination of the alkoxy ligands.[27−29] Increasing the size of one of the two (X and Y) ligands also favors **M-TBP**: highly bulky phenoxy ligands take the apical site in a TBP metallocyclobutane.[31−33] The E group that is multiply bonded to the metal also plays a role: replacing the imido group by an oxo group favors the SP structure.[34,35]

Computational studies on the metallacyclobutanes derived from the Schrock-type catalysts have been carried out with models of ligands mimicking the electronic properties of the real ligands.[12−15,23,39−48] A seminal DFT study by Folga and Ziegler on a simple model of molybdacyclobutane, [Mo(E)-(C_3H_6)X_2] with E = NH and O and X = Cl, OCH_3, and OCF_3, has shown that (i) the metallacyclobutane ring is planar and folded in the TBP and SP isomers, respectively, and that (ii) the preference for a TBP structure increases with the electron-withdrawing character of X.[40] Metallacylobutanes were calculated to have a general preference for a SP structure for a set of Mo, W, and Re complexes with nonbulky alkyl, pyrrolyl, alkoxy, and siloxy ligands.[12−15,23,47] Related studies in the alkyne metathesis reactions have identified metallacyclobutadiene intermediates whose structural features were discussed.[49−52]

Here, we used DFT calculations to explore the structural preferences (TBP vs SP) of nonsubstituted metallacyclobutanes of the general formula M(E)(C_3H_6)(X)(Y) with M = Mo and W, and E = aryl-imido, alkyl-imido, or oxo, and X/Y are a wide variety of anionic ligands such as alkyl, alkoxy, fluoroalkoxy, pyrrolyl, dimethylpyrrolyl and the large phenoxy ligands that have been experimentally used. By carrying out this computational study on a large set of ligands, we aim at rationalizing the factors that determine the preference for **M-TBP** vs **M-SP** isomeric forms. Toward this goal, we first evaluated the structural features and NMR signatures as a function of E, X, and Y. Next, we studied the stability of **M-TBP** and **M-SP** relative to the separated reactants (methylidene complex M(E)(=CH_2)(X)(Y) and ethene) and related it in a qualitative manner to the structure and the relative stability of the observed metallacyclobutanes. Finally, we computed the energy barriers for the TBP-SP interconversion for some selected systems and discuss how these barriers influence the alkene metathesis process.

■ COMPUTATIONAL DETAILS

Calculations were carried out with the hybrid B3PW91[53,54] and M06[55] density functionals. While the two methods give similar trends, the results with M06 are in better agreement with the available experimental data (see below) and are used for discussing the results. The Mo and W atoms were represented with the quasi relativistic effective core pseudopotentials (RECP) of the Stuttgart group and the associated basis sets augmented with a polarization function.[56−59] The remaining atoms (H, C, N, O, and F) were represented with 6-31G(d,p) basis sets.[60] Geometry optimizations were performed without any symmetry constraint, and vibrational analysis was used to verify that the resulting geometry is a minimum on the potential energy surface. Values given along the text are based on gas phase Gibbs energies calculated within the harmonic approximation at 298 K and 1 atm and using the separated reactants (methylidene complex and ethene) as reference. The solvent (toluene, usually used for NMR measurement) influence was evaluated with the SMD method[61] as single point calculations on the M06 structures. The Gibbs energy is calculated as the sum of the energies calculated in the solvent and the entropic contribution calculated in the gas phase. All calculations were performed with the Gaussian 09 package.[62]

The ^{1}H and ^{13}C NMR chemical shifts as well as J_{CH} coupling constants were calculated with the B3PW91 and M06 functionals using the GIAO method.[63] Similar results were obtained with the two functionals, but we report only those with M06. In these calculations, the main group elements were represented with the IGLO-II basis set,[64] while Mo and W were represented with the ECP and basis set used for the geometry optimization. This methodology was shown previously to give reasonable chemical shifts and J_{CH} coupling constants for related systems.[65−67] The natural population analysis (NPA) charges of Weinhold et al.[68] and the atoms in molecules analysis (AIM) of Bader[69] were used to analyze the bonding.

DOI: 10.1021/acs.organomet.5b00147
Organometallics 2015, 34, 1668−1680

Scheme 2. Methylidene Complexes Used for the Study of the Corresponding Metallacyclobutanes

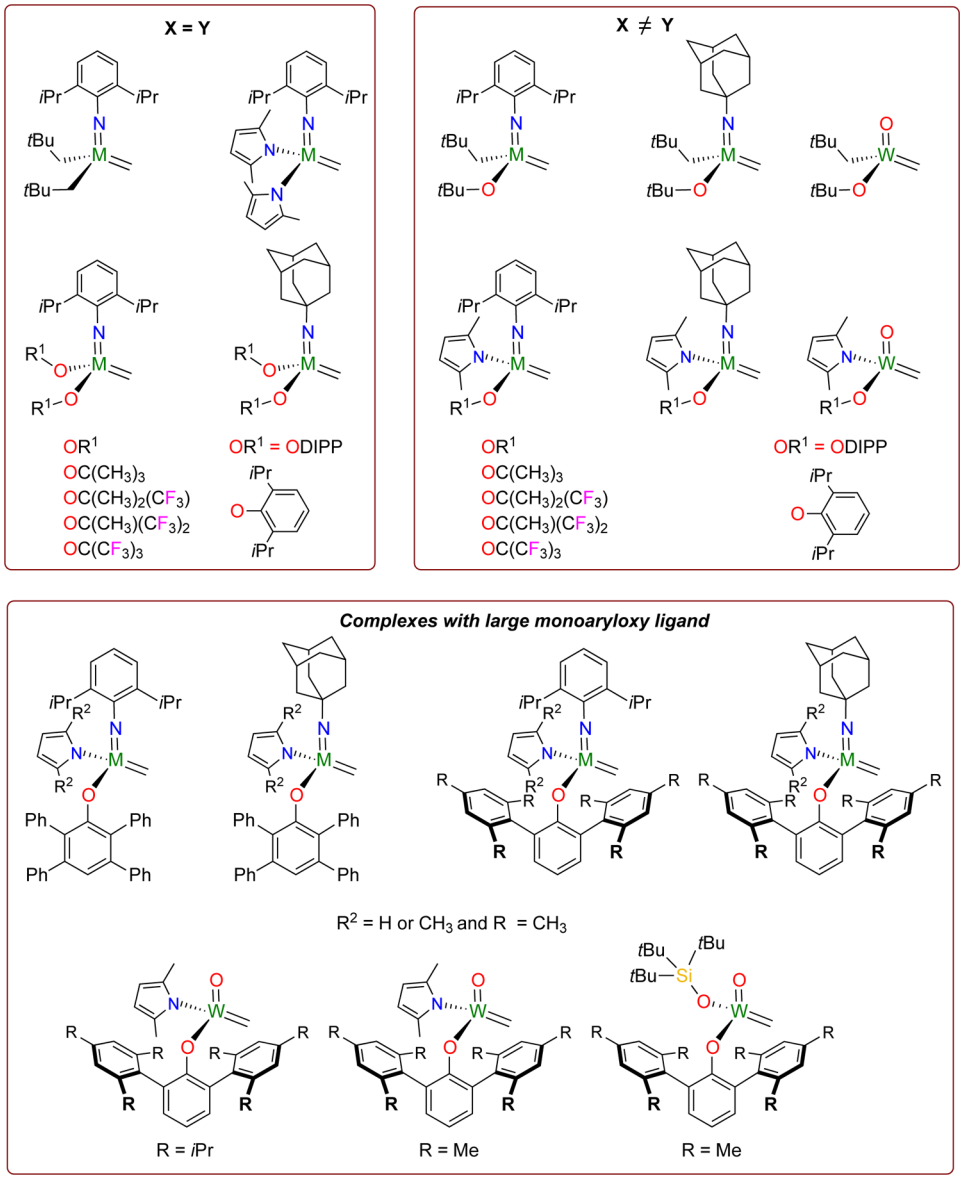

For the complexes with large ligands such as 2,3,5,6-tetraphenylphenoxy, (OTPP), and 2,6-di(2,4,6-tris-isopropyl)phenoxy, (HIPTO), the solid-state structures were used as initial guesses for the geometry optimization. In most cases, this information available for one isomer only, is used to initiate the optimization for the other isomer. These large ligands did not appear to have large conformational complexity, unlike smaller ligands like the fluorinated *tert*-butoxy derivatives. For these latter systems, a conformational search was carried out in order to obtain the most stable conformation.

RESULTS AND DISCUSSION

Systems Considered. As mentioned earlier, the complexes considered hereafter correspond to some of the most significant and representative examples discussed in the literature and are calculated by including the real ligands.[26−29,31−35] Only the nonsubstituted metallacyclobutanes (M = Mo and W), derived from the addition of ethene to the methylidene complexes, were calculated (Scheme 2). The E, X, and Y ligands in the methylidene complexes are organized in three groups: (i) Complexes with identical X- and Y-ligands in which X = Y = neopentyl (CH_2tBu); 2,5-dimethylpyrrolyl (Me_2Pyr); or some of the common alkoxy derivatives $OC(CH_3)_3$, $OC(CH_3)_2CF_3$, $OC(CH_3)(CF_3)_2$, $OC(CF_3)_3$ (labeled as O*t*Bu, $OtBu_{F3}$, $OtBu_{F6}$, and $OtBu_{F9}$, respectively), and 2,6-di-isopropylphenoxy (ODIPP). In this set, the E ligand is an alkyl and aryl imido ligand. (ii) Complexes with different X- and Y-ligands for which X is CH_2tBu or Me_2Pyr, and Y is one of the alkoxy and phenoxy ligands mentioned above (O*t*Bu, $OtBu_{F3}$, $OtBu_{F6}$, or ODIPP). In these complexes, the most donating ligand is at the equatorial site of the TBP as this is known to be preferred.[13] In this set, the E ligand is an alkyl, aryl imido, and oxo ligand. (iii) Complexes with one large monoaryloxy ligand as Y; 2,3,5,6-tetraphenylphenoxy (OTPP), 2,6-di(2,4,6-tris-isopropylphenyl)phenoxy (HIPTO), and 2,6-di(2,4,6-trismethyl)phenoxy (HIMTO); and pyrrolyl (Pyr), dimethyl pyrrolyl (Me_2Pyr), and siloxy group as the X ligand. In this set, the E ligand is an alkyl, aryl imido, or oxo ligand.

Structural Features of M-TBP and M-SP. Two TBP metallacyclobutanes, $W(NAr)(C_3H_6)(Me_2Pyr)(OTPP)$[31] and $W(NAr)(C_3H_6)(Pyr)(HIPTO)$,[32] and one SP metallacyclobutane, $W(O)(C_3H_6)(OSi(tBu)_3)(HIMTO)$,[35] whose structures

DOI: 10.1021/acs.organomet.5b00147
Organometallics 2015, 34, 1668−1680

were determined by X-ray diffraction, were used to validate the computational level. Table 1 shows that B3PW91 and M06

Table 1. Calculated and Solid-State Structural Parameters (Distances *d* in Å and Angles *θ* and Torsional Angles Ω in Degrees) of Selected Metallacyclobutanes

structural data	M06	B3PW91	X-ray
W(NAr)(C_3H_6)(Me_2Pyr)(OTPP), TBP Structure[31]			
d(M-E) E = NAr	1.762	1.768	1.7676(7)
d(M-X) X = Me_2Pyr	2.066	2.063	2.0581(18)
d(M-Y) Y = OTPP	1.993	1.989	1.9703(15)
d(M-C_α)/ d(M-$C_{\alpha'}$	2.056/2.068	2.057/2.069	2.057(2)/2.058(2)
d(C_α-C_β)/ d($C_{\alpha'}$-C_β)	1.593/1.585	1.595/1.587	1.603(3)/1.597(3)
d(M-C_β)	2.369	2.382	2.368(2)
θ (C_α-C_β-$C_{\alpha'}$)	117.9	117.2	117.44(18)
θ (C_α-M-$C_{\alpha'}$)	82.6	82.3	83.3
Ω(C_α-M-$C_{\alpha'}$-C_β)	0.3	0.2	0.88(18)
W(NAr)(C_3H_6)(Pyr)(HIPTO), TBP Structure[32]			
d(M-E) E = NAr	1.756	1.765	1.768(7)
d(M-X) X = Pyr	2.073	2.060	2.058(8)
d(M-Y) Y = HIPTO	1.978	1.977	1.980(6)
d(M-C_α)/ d(M-$C_{\alpha'}$)	2.066/2.059	2.067/2.064	2.037(9)/2.038(10)
d(C_α-C_β)/ d($C_{\alpha'}$-C_β)	1.592/1.593	1.592/1.595	1.635(14)/ 1.588(14)
d(M-C_β)	2.360	2.375	2.380(9)
θ (C_α-C_β-$C_{\alpha'}$)	118.4	117.7	115.2(7)
θ (C_α-M-$C_{\alpha'}$)	83.0	82.6	83.8(4)
Ω(C_α-M-$C_{\alpha'}$-C_β)	1.4	0.0	1.73
W(O)(C_3H_6)(OSi(*t*Bu)$_3$)(HIMTO), SP Structure[35]			
d(M-E) E = O	1.691	1.693	1.690(2)
d(M-X) X = OSi(*t*Bu)$_3$	1.876	1.877	1.875(3)
d(M-Y) Y = HIMTO	1.909	1.918	1.896(2)
d(M-C_α)/ d(M-$C_{\alpha'}$	2.170/2.174	2.177/2.179	2.168(3)/2.172(3)
d(C_α-C_β)/ d($C_{\alpha'}$-C_β)	1.520/1.522	1.525/1.526	1.522(4)/1.527(4)
d(M-C_β)	2.761	2.777	2.762
θ (C_α-C_β-$C_{\alpha'}$)	95.7	95.7	96.5(2)
θ (C_α-M-$C_{\alpha'}$)	62.6	62.6	62.7(1)
Ω(C_α-M-$C_{\alpha'}$-C_β)	22.3	21.5	22.0

reproduce well the geometrical features of these three metallacyclobutanes, with differences between the computed and experimental structural parameters being less than 0.04 Å for bond distances and 3.5° for bond angles. Therefore, both methods can be used for structural assignment. In particular, the calculations reproduce the observed conformational preferences of 2,5-dimethylpyrrolyl (Me_2Pyr) vs nonsubstituted pyrrolyl (Pyr) as shown in Figure 1 (top and middle structures). While Pyr is perpendicular to the plane containing the metallacyclobutane, Me_2Pyr is significantly twisted relative to the ring, presumably due to the steric interaction between the methyl groups and the bulky substituent of the imido group. While the geometries are very similar with the two methods, calculated relative M06 energies of **M-TBP** and **M-SP** are in better agreement with the experimental preferences (*vide infra*); we consequently discuss the results based on calculations with the M06 functional. Structural information on all calculated complexes are given in the Supporting Information (Tables S5−S22).

The calculations carried out for the metallacyclobutanes derived from the alkylidene complexes of Scheme 2 show that the salient features of **M-TBP** and **M-SP** are not sensitive to the nature of the metal, the E, and/or X/Y ligands (Table 2 and

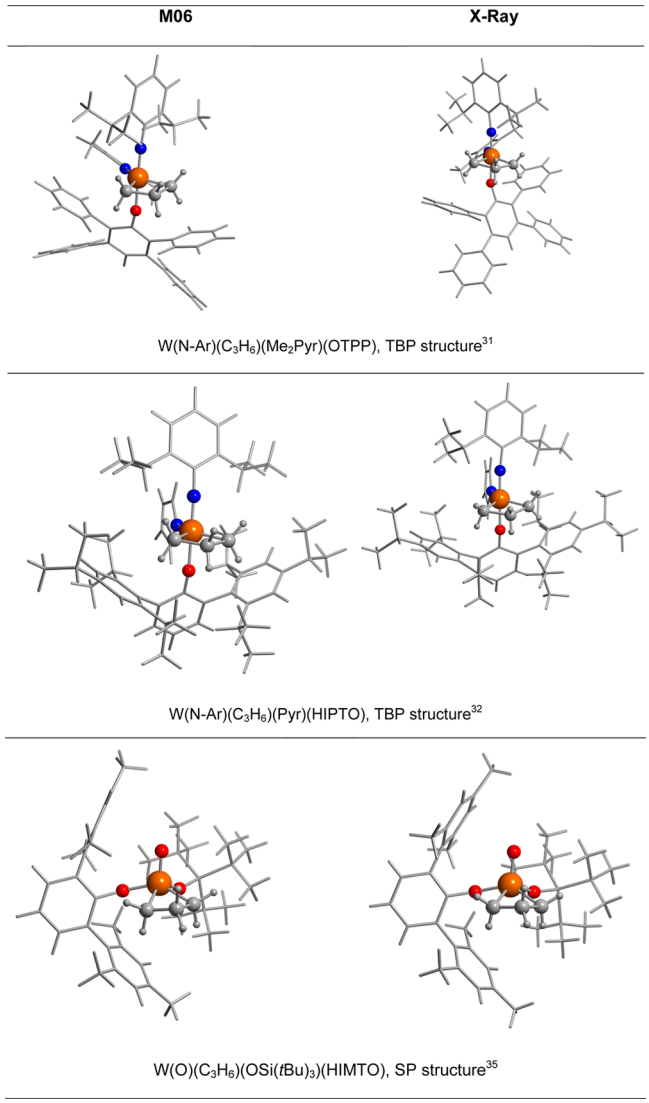

Figure 1. M06 optimized (left) and solid-state structures (right) of selected **M-TBP** and **M-SP**.

Tables S5−S22, Supporting Information). The main features of these metallacyclobutanes reside in their shapes, which is planar for **M-TBP** and folded for **M-SP**. Figure 2 illustrates this aspect by showing the first coordination sphere for W(NAr)(C_3H_6)-(O*t*Bu_{F6})$_2$. Table 2 shows that the range for the torsional angle Ω that characterizes these rings is small, 0−8° and 23−30° for **M-TBP** and **M-SP**, respectively. The bond distances within the metallacyclobutane ring are also distinctively different in the two isomers. In **M-TBP**, the M-C_α bond distances are short (2.04−2.12 Å), the C−C bond distances are long (1.57−1.61 Å), and there is a rather short M···C_β distance (2.33−2.43 Å). These features translate into angles (C_α-M-$C_{\alpha'}$) and (C_α-C_β-$C_{\alpha'}$) of 81−84° and 116−118°, respectively. In **M-SP**, the M-C_α bonds are longer (2.15−2.20 Å), the C_α-C_β bonds are shorter (1.51−1.52 Å), and the M···C_β is much longer (2.75−2.81 Å). As a result, the angles (C_α-M-$C_{\alpha'}$) of 61−63° and (C_α-C_β-$C_{\alpha'}$) of 93−97° are more acute in **M-SP** than in **M-TBP**.

Table 2 also shows structural features associated with the metal−ligand bond distances other than M-carbon. The bond distances between the metal and the multiply bonded E ligand (imido or oxo) are systematically longer for **M-TBP** than for **M-SP**. This is also the case for M-X and M-Y bond distances

DOI: 10.1021/acs.organomet.5b00147
Organometallics 2015, 34, 1668−1680

Table 2. Range in the Calculated Structural Parameters in M-TBP and M-SP[a]

	M-TBP		M-SP	
structural parameters	Mo	W	Mo	W
d(M-E) E = NAr	1.73−1.76	1.75−1.78	1.70−1.73	1.72−1.75
d(M-E) E = NAd	1.71−1.74	1.74−1.76	1.68−1.71	1.71−1.73
d(M-E) E = O	N.A.	1.71−1.72	N.A.	1.69
d(M-C_α)	2.04−2.09	2.05−2.12	2.15−2.20	2.16−2.20
d(C_α-C_β)	1.57−1.60	1.57−1.61	1.51−1.52	1.52
d(M-C_β)	2.33−2.41	2.35−2.43	2.76−2.81	2.75−2.80
θ(C_α-C_β-$C_{\alpha'}$)	116−118	116−118	93−96	94−97
θ(C_α-M-$C_{\alpha'}$)	81−83	81−84	61−63	61−63
Ω(C_α-M-$C_{\alpha'}$-C_β)	0−7	0−8	24−29	23−30

[a]Distances d are in Å; angles θ and torsional angles Ω are in degrees.

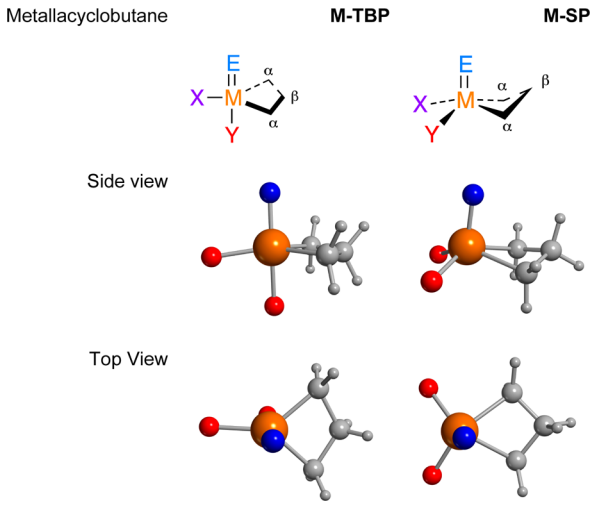

Figure 2. First coordination sphere of W(NAr)(C_3H_6)($OtBu_{F6}$)$_2$ in **M-TBP** (left) and **M-SP** (right).

(Tables S5−S22, Supporting Information). The replacement of the aryl-imido by an alkyl-imido ligand leads to shorter M-NR bond distances and slightly longer M-X and M-Y bonds in all species (**M-TBP**, **M-SP**). Moreover, the M-X and M-Y bond distances are further lengthened by replacing the imido by the oxo ligand. These facts are consistent with alkyl-imido being more electron donating than aryl-imido one and the oxo acting as the strongest of all as already mentioned when using simplified models.[15]

The specific structural features of the metallacyclobutane ring in the **M-TBP** and **M-SP** complexes can be rationalized by performing a molecular orbital analysis as already noted by Folga and Ziegler.[40] A convenient way to carry out this analysis is to consider that the metallacyclobutane is formed by combining a metallic fragment $[ML_3]^{2+}$ and an organic fragment $[C_3H_6]^{2-}$. With this convention, all d orbitals are empty for both metal fragments.[70] *mer* and *fac* $[ML_3]^{2+}$ fragments are used to build **M-TBP** and **M-SP**, respectively.

The key molecular orbitals of the two fragments, which are used for constructing the whole metallacyclobutane complexes, are shown in Figure 3, in the C_s symmetry point group. The organic fragment uses an in-phase (σ^+) and an out-of-phase (σ^-) combination of lone pairs of the terminal anionic carbons. The *mer* $[ML_3]^{2+}$ fragment has three nonbonding d orbitals (d_{1b}, d_{1a}, and d_{2b}) and just above a d_{2a} orbital. The *fac*-fragment has also three low-lying essentially nonbonding d orbitals (d_{1a},

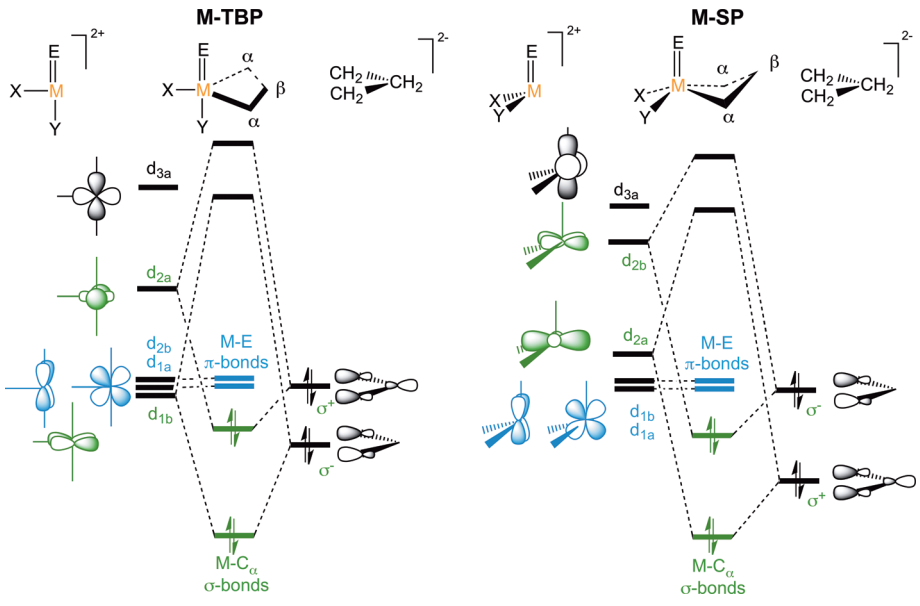

Figure 3. Qualitative interaction diagram for the interaction of $[M(E)(X)(Y)]^{2+}$ and $[C_3H_6]^{2-}$ to form the metallacyclobutane. Left, *mer* metal fragment for forming **M-TBP**; right, *fac* metal fragment for forming **M-SP**.

DOI: 10.1021/acs.organomet.5b00147
Organometallics 2015, 34, 1668−1680

Table 3. Calculated and Experimental ^{1}H and ^{13}C NMR Chemical shifts, in ppm, for Selected W Metallacyclobutanes

				H_α		H_β		C_α		C_β	
E	X	Y	type	cal[a]	exp	cal[a]	exp	cal[a]	exp	cal[a]	Exp
NAr	O*t*Bu	O*t*Bu	SP[28]	1.4	2.3	2.4	4.4	37.1	41.9	27.4	24.5
					2.8						
NAr	$OtBu_{F3}$	$OtBu_{F3}$	TBP[28]	4.5	4.6	0.3	−0.7	88.0	98.8	−4.2	−3.6[b]
					4.4		−1.2				
NAr	$OtBu_{F3}$	$OtBu_{F3}$	SP[28]	1.5	2.2	2.4	4.3	39.8	43.6	27.4	24.2
							2.8				
NAr	ODIPP	ODIPP	TBP[28]	4.5	4.9	0.2	−0.6	91.7	95.5	−4.0	−1.9
					4.7		−1.0				
NAr	ODIPP	ODIPP	SP[28]	1.5	2.3	2.4	4.4	39.4	43.5	26.5	22.6
NAr	Me_2Pyr	OTPP	TBP[31]	3.8	4.3	0.2	−0.9	94.7	101.	−3.0	−3.5
					3.3		−1.4				
NAr	Pyr	HIPTO	TBP[32]	3.5	4.2	−0.1	−0.8	93.2	98.6	−4.4	−3.7
					3.5		−1.1				
O	HIMTO	$OSitBu_3$	SP[35]	0.9	1.9	2.0	4.1	37.5	43.8	25.0	22.3
					2.5				41.4		

[a]Average values. [b]The value of −3.6 is that in Figure 3 and not in the text (3.6).[28]

d_{1b}, and d_{2a}) below a d_{2b} orbital. In each isomer, two metal d orbitals are involved in the M−E σ-interactions (d_{1a} and d_{2b} for **M-TBP** and d_{1a} and d_{1b} for **M-SP**), leaving two metal d orbitals still available for interacting with the organic fragment $[C_3H_6]^{2-}$ in both cases. As already pointed out by Folga and Ziegler, increasing the interaction between d_{2a} and σ^+ in **M-TBP** favors large C_α-C_β-$C_{\alpha'}$ and C_α-M-$C_{\alpha'}$ angles. In contrast, in **M-SP**, the M-C bonding is dominated by the interaction between d_{2b} and σ^-, which favors more acute C_α-C_β-$C_{\alpha'}$ and C_α-M-$C_{\alpha'}$ angles.[40] The shapes of the two metallacyclobutanes are the (sole) result of the interaction between the frontier orbitals of the metal and organic fragment whose overlap is determined by the metal−C_α interactions. Worthy of note, the calculations do not identify any direct interaction between the metal and C_β.[71] An NBO analysis, carried out for W(NAr)-$(C_3H_6)(OtBu_{F6})_2$, shows total charges of −0.03 and −0.36 on the C_3H_6 moiety in the TBP and SP isomers, respectively. The organic fragment is significantly more electron poor in the TBP isomer, which probably also correlates with longer C−C and shorter M-C bonds and accounts for the TBP isomer being on the metathesis pathway.

^{1}H and ^{13}C NMR Signatures of M-TBP and M-SP. The calculated ^{1}H and ^{13}C NMR chemical shifts for selected **W-TBP** and **W-SP** metallacyclobutanes are compared to the experimental values in Table 3.[72] There is a reasonably good agreement between calculated and experimental chemical shifts with a difference of less than 1.6 and 4.0 ppm for ^{1}H and C_β, respectively. The differences are higher for C_α (ranging from 3.8 to 10.8 and in general less than 6.0 ppm). The larger deviations at C_α are most likely due to the lack of inclusion of the spin−orbit coupling particularly important in a direct contact between the two atoms.[73−76] Yet, the calculations very nicely reproduce the trends of ^{13}C NMR signatures of **M-TBP** vs **M-SP**. Typically for **M-SP**, C_α and C_β have chemical shifts around 40 and 25 ppm, respectively, while for **M-TBP**, the corresponding values are around 90 and −3 ppm. These values are not significantly affected by the chemical nature of the ancillary ligands (Tables S23 to S29 of the Supporting Information). The presence of fluorine atoms in the alkoxy groups increases the chemical shifts of the C_α carbons. A similar effect on the chemical shifts of the C_α carbons is observed when substituting the more donor alkyl imido by the less donor aryl imido group. These data are consistent with a larger electron donation from the C_α carbons to the metal when E-, X-, and Y-ligands are weaker donors. Likewise, the J_{CH} coupling constants, calculated for the C_α and C_β centers of the metallacyclobutane ring in the SP and TBP isomers, agree well with the experimental data (Tables S30 to S33 of the Supporting Information).

Energetics of M-TBP and M-SP. *Validation.* The relative energies of **M-SP** and **M-TBP** as well as their stabilities with respect to the separated reactants are described as a function of M, E, X, and Y for the set of species presented in Scheme 2. Validation of the method was achieved by comparing the energetics calculated with B3PW91 and M06 for selected metallacyclobutanes that were experimentally observed and whose ratio, probably associated with the thermodynamic equilibrium, was reported (Table 4). Negatives values for the free energies of formation of the metallacyclobutane relative to the methylidene complex (ΔG) and ethene indicate that the metallacyclobutane should be more stable than the reactants and could be in principle observed. Indeed, for all observed species, the calculations with either functional give a negative ΔG. However, the two functionals differ slightly in predicting the more stable isomer as indicated by Δ(TBP-SP), which is positive when **M-SP** is more stable. For instance, for entries 1 and 9, both functionals give a preference for **W-SP** in agreement with the sole observation of this isomer. For entry 2, both isomers have been observed, and this fits better with the small Δ(TBP-SP) of 0.5 kcal/mol (M06) than the value of 3.6 kcal/mol obtained with B3PW91. For entry 3, only M06 gives the preference for **W-TBP** as expected from the experimental data. Similar behavior is obtained for entries 5 to 8. The only exception is found in entry 4, for which **Mo-TBP** has been the only observed isomer, while M06 calculations give essentially the same energy for the two isomers. Overall, the calculated data shows that M06 reproduces slightly better the experimental observation than B3PW91 by stabilizing **M-TBP** over **M-SP** more than B3PW91 for any set of ligands. Consequently, only the results with the M06 functional will be presented hereafter.[77]

Energetics of the Metallacyclobutanes with X = Y. The Gibbs free energies (ΔG) of the symmetric (X = Y) aryl imido metallacyclobutanes are given relative to the separated

DOI: 10.1021/acs.organomet.5b00147
Organometallics 2015, 34, 1668−1680

Table 4. Energies and Gibbs Free Energies in kcal/mol of M-TBP and M-SP Relative to the Separated Methylidene Complex and Ethene

Entry	Alkylidene	Isomer	B3PW91		M06		Exp.
			ΔE	ΔG	ΔE	ΔG	
1	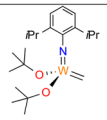	TBP	-14.7	4.1	-23.7	-5.9	
		SP	-22.2	-4.5	-28.8	-10.2	
		Δ(TBP-SP)	7.5	8.7	5.1	4.3	SP[28]
2	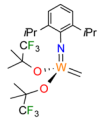	TBP	-20.9	-2.7	-27.5	-10.3	
		SP	-22.9	-6.3	-29.4	-10.8	
		Δ(TBP-SP)	2.0	3.6	2.0	0.5	SP +TBP[28]
3	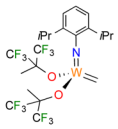	TBP	-22.6	-4.1	-31.6	-13.9	
		SP	-23.1	-5.0	-31.4	-10.8	
		Δ(TBP-SP)	0.6	0.9	-0.2	-3.1	TBP[28]
4	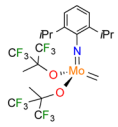	TBP	-16.3	1.7	-25.5	-8.8	
		SP	-19.0	-0.8	-27.6	-9.7	
		Δ(TBP-SP)	2.6	2.5	2.1	0.8	TBP[29]
5	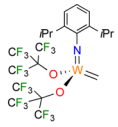	TBP	-24.7	-5.1	-35.1	-15.6	
		SP	-23.4	-6.3	-31.8	-9.9	
		Δ(TBP-SP)	-1.3	1.2	-3.2	-5.7	TBP[28]
6	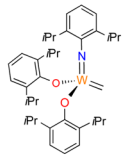	TBP	-21.0	-0.7	-28.7	-12.3	
		SP	-22.0	-3.8	-31.9	-14.4	
		Δ(TBP-SP)	1.0	3.1	3.2	2.2	SP + TBP[28]
7	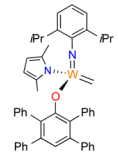	TBP	-17.6	0.0	-26.5	-11.3	
		SP	-14.9	3.0	-26.4	-9.3	
		Δ(TBP-SP)	-2.7	-3.0	-0.1	-2.0	TBP[31]
8	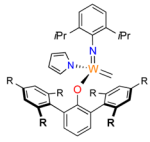	TBP	-22.1	-2.7	-29.0	-9.7	
		SP	-15.9	2.3	-25.2	-7.9	
		Δ(TBP-SP)	-6.3	-5.0	-3.7	-1.8	TBP[32]
9		TBP	-11.7	+8.2	-22.7	-5.2	
		SP	-22.3	-4.0	-30.0	-12.5	
		Δ(TBP-SP)	+10.5	+12.2	+7.3	+7.3	SP[35]

reactants, i.e., the separated methylidene complex and ethene (Table 5). The results for the adamantyl imido species are given in the Supporting Information (Table S1).

For any set of ligands, W increases the stability of the metallacyclobutanes by as much as 8 kcal/mol compared to Mo. This is consistent with the general observation that tungstena are more stable than molybdenacyclobutanes. In general, electron withdrawing X and Y ligands (decreasing σ-donating ability) increase the stability of the two forms of the metallacyclobutane for either Mo or W. Conversely electron donating X and Y ligands destabilize the two isomers and significantly more **M-TBP**. This leads to an influence of the X and Y ligands on the relative energy of **M-TBP** and **M-SP**. The strongest preference for **M-TBP** is for X = Y = O*t*Bu$_{F6}$ and O*t*Bu$_{F9}$ with W (Entries 12 and 13) and the strongest preference for **M-SP** is for X = Y = CH$_2$*t*Bu or dimethylpyrrolyl with the two metals (entries 1 and 2 and 8 and 9). Increasing the donating ability of the imido ligand (alkyl imido vs aryl imido) has a similar destabilizing effect on **M-TBP** relative to **M-SP** (see Supporting Information). These computed trends are in agreement with experiments: (i) W(NR)(C$_3$H$_6$)(O*t*Bu)$_2$ has been observed solely as a square-pyramidal isomer by NMR spectroscopy.[28] (ii) A mixture of SP and TBP isomers is observed for W(NR)(C$_3$H$_6$)(O*t*Bu$_{F3}$)$_2$. (iii) **W-TBP** has been the only detected isomer for W(NR)(C$_3$H$_6$)(O*t*Bu$_{F6}$)$_2$ and W(NR)(C$_3$H$_6$)(O*t*Bu$_{F9}$)$_2$.[28] (iv) ODIPP behaves like O*t*Bu$_{F3}$ (similar Δ(TBP-SP), which nicely agrees with experiments that indicate a mixture of SP and TBP isomers.

Energetics of the Dissymmetric (X≠Y) Metallacyclobutanes. Results for a series of complexes for M = Mo or W, E = NAr, NAd, or O, X = Me$_2$Pyr or CH$_2$*t*Bu, and Y = O-bound ligands defined above (O*t*Bu$_{F0-6}$ and ODIPP) are presented in Table 6. The results for the related adamantyl imido and oxo species are shown in Tables 7 and S2, Supporting Information.

Replacing one of the alkoxy ligands by a more electron donating one (Me$_2$Pyr or CH$_2$*t*Bu) decreases the stability of the metallacyclobutane. Trends identified for symmetric systems (X = Y) are also valid for the dissymmetric complexes. For NR = aryl and adamantyl and X = Me$_2$Pyr or CH$_2$*t*Bu, (i) W gives more stable metallacyclobutanes with respect to separated reactants than Mo regardless of the nature of X and Y ligands, and (ii) there is a general preference for **M-SP** over **M-TBP** when the Y ligand has no fluorine atoms. This preference is higher for Mo than for W and for alkyl imido than for the aryl imido, and (iii) there is a preference for **M-TBP** when Y is a weak electron donating ligand such as O*t*Bu$_{F6}$. Therefore, there is a modest influence of the nature of X on the TBP vs SP isomeric preference.

In the case of the tungsten oxo metallacyclobutanes, **W-TBP** is destabilized relative to **W-SP** and to the separated reactants. As a result, there is a clear energetic preference for the **W-SP** isomer over **W-TBP**. This preference is not reversed with the most electron withdrawing ligands such as the fluoro alkoxy Y ligands (Δ(TBP-SP) > 5 kcal mol^{-1}). Overall, calculations suggest that oxo **W-TBP** should not be observed, while W-SP isomers should, which is consistent with recent reports.[34,35,78−81]

Energetics of the Large Mono Aryloxy Pyrrolyl (MAP) Metallacyclobutanes. A series of MAP complexes with aryloxy ligands of different sizes, reproducing some of the recently used experimental ligands, have been computed (E = *N*-2,6-di-isopropylphenyl, *N*-adamantyl or oxo; X = Pyr or Me$_2$Pyr and Y = ODIPP, OTPP, HIPTO, or HIMTO).[31−33] Table 8 (E = *N*-2,6-di-isopropylphenyl and X = Me$_2$Pyr), Table S3 (Supporting Information) (E = *N*-2,6-di-isopropylphenyl and X = Pyr), and Table S4 (Supporting Information) (E = *N*-adamantyl or oxo) report the Gibbs energy (ΔG) associated with the formation of **M-TBP** and **M-SP** from [M(E)(=CH$_2$)(X)(Y)] and ethene as well as the difference of Gibbs energies between **M-TBP** vs **M-SPY**.

For the aryl- and alkyl-imido species, the calculations show that the larger aryloxy ligands (ODIPP < OTPP < HIPTO) slightly destabilize the metallacyclobutanes (TBP as well as SP)

DOI: 10.1021/acs.organomet.5b00147
Organometallics 2015, 34, 1668−1680

Table 5. M06(SMD) Gibbs Free Energies in kcal/mol of the Symmetric (X = Y) M(NAr)(C_3H_6)(X)(Y) Complexes[a]

entry	M	X	Y	ΔG M-TBP[b]	ΔG M-SP[b]	Δ(TBP-SP)[c]	exp
1	Mo	CH_2tBu	CH_2tBu	7.6	−2.5	10.1	
2	Mo	Me_2Pyr	Me_2Pyr	4.7	−2.1	6.7	
3	Mo	O*t*Bu	O*t*Bu	−2.3	−8.2	5.9	
4	Mo	O*t*Bu$_{F3}$	O*t*Bu$_{F3}$	−3.7	−5.8	2.2	
5	Mo	O*t*Bu$_{F6}$	O*t*Bu$_{F6}$	−8.8	−9.7	0.8	TBP[29]
6	Mo	O*t*Bu$_{F9}$	O*t*Bu$_{F9}$	−7.6	−6.4	−1.1	
7	Mo	ODIPP	ODIPP	−5.4	−8.3	3.0	
8	W	CH_2tBu	CH_2tBu	6.6	0.3	6.3	
9	W	Me_2Pyr	Me_2Pyr	0.6	−4.3	4.8	
10	W	O*t*Bu	O*t*Bu	−5.9	−10.2	4.3	SP[28]
11	W	O*t*Bu$_{F3}$	O*t*Bu$_{F3}$	−10.3	−10.8	0.5	SP+TBP[28]
12	W	O*t*Bu$_{F6}$	O*t*Bu$_{F6}$	−13.9	−10.8	−3.1	TBP[28]
13	W	O*t*Bu$_{F9}$	O*t*Bu$_{F9}$	−15.6	−9.9	−5.7	TBP[28]
14	W	ODIPP	ODIPP	−12.3	−14.4	2.1	SP+TBP[28]

[a]Δ*G* is the Gibbs free energies relative to the separated alkylidene complex and ethene. Δ(TBP-SP) is the difference in Gibbs free energies between **M-TBP** and **M-SP**. [b]A positive value for ΔG means that the metallacyclobutane is higher in energy than the separated reactants (methylidene complex and ethene). [c]A positive value means that **M-SP** is preferred over **M-TBP**.

Table 6. M06(SMD) Gibbs Energies in kcal/mol of the Dissymmetric (X ≠ Y) M(NAr)(C_3H_6)(X)(Y) Complexes[a]

entry	M	X	Y	ΔG M-TBP[b]	ΔG M-SP[b]	Δ(TBP-SP)[c]
1	Mo	Me_2Pyr	O*t*Bu	−3.5	*−7.0*	3.4
2	Mo	Me_2Pyr	O*t*Bu$_{F3}$	*−6.5*	*−5.4*	*−1.1*
3	Mo	Me_2Pyr	O*t*Bu$_{F6}$	*−3.1*	−3.7	0.5
4	Mo	Me_2Pyr	ODIPP	−9.6	−8.7	−0.9
5	W	Me_2Pyr	OtBu	*−7.4*	−8.6	1.2
6	W	Me_2Pyr	O*t*Bu$_{F3}$	*−11.3*	−10.0	−1.3
7	W	Me_2Pyr	O*t*Bu$_{F6}$	−8.0	−7.8	−0.2
8	W	Me_2Pyr	ODIPP	−11.5	−10.5	−1.0
9	Mo	CH_2tBu	O*t*Bu	−2.9	−7.3	+4.4
10	Mo	CH_2tBu	O*t*Bu$_{F3}$	−4.9	−5.6	+0.7
11	Mo	CH_2tBu	O*t*Bu$_{F6}$	−5.7	−6.6	+0.9
12	Mo	CH_2tBu	ODIPP	−4.6	−4.2	−0.4
13	W	CH_2tBu	O*t*Bu	*−4.4*	−7.1	+2.7
14	W	CH_2tBu	O*t*Bu$_{F3}$	−11.2	−5.6	−5.6
15	W	CH_2tBu	O*t*Bu$_{F6}$	−8.5	−6.7	−1.8
16	W	CH_2tBu	ODIPP	−7.1	−5.2	−1.9

[a]ΔG is the Gibbs free energy relative to the separated methylidene complex and ethene. Δ(TBP-SP) is the difference in Gibbs free energy between **M-TBP** and **M-SP**. [b]A positive value for ΔG means that the metallacyclobutane is higher in energy than the separated reactants. [c]A positive value means that **M-SP** is preferred over **M-TBP**.

relative to the separated methylidene complex and ethene. The influence of the metal center is similar to what was found before so that *W*-metallacyclobutanes are more stable than their Mo-equivalents. Replacing aryl-imido by adamantyl imido (or oxo) slightly (or strongly) destabilizes the metallacyclobutane and favors **M-SP** over **M-TBP**. Increasing the size of the ligand (ODIPP < OTPP < HIPTO) with similar electron withdrawing character favors **M-TBP** over **M-SP** geometry, and this finding is fully consistent with the observation of only **Mo-TBP** and **W-TBP** with large phenoxy ligands.[31−33] We have analyzed the effect of replacing Me_2Pyr (Table 8) by Pyr (Table S3, Supporting Information) for this set of ligands. The calculations show that the formation of metallacyclobutanes is more favorable with the latter, but it is not clear how Pyr influences the difference between **M-TBP** and **M-SP**, showing again a modest influence of the X ligand on the **M-TBP** vs **M-SP** isomeric preference.

In summary, some trends appear from this extensive study. The stability of the metallacyclobutane relative to the separated reactants (methylidene complex plus ethene) is larger for W than Mo and is increased by the presence of electron withdrawing ligands. **M-SP** is preferred over **M-TBP**, when E is an oxo or an adamantyl ligand, and when X and Y are both strong electron donating groups such as alkyl, pyrrolyl, or O*t*Bu ligands. E- and Y-ligands appear to have a leading influence on the **M-TBP**/**M-SP** preference. In particular, weak electron donating E and Y ligands favor **M-TBP**. Therefore, **M-TBP**

Table 7. M06(SMD) Gibbs Energies in kcal/mol of Dissymmetric (X ≠ Y) M(E)(C_3H_6)(X)(Y) Complexes[a]

entry	M	E	X	Y	ΔG M-TBP[b]	ΔG M-SP[b]	Δ(TBP-SP)[c]
1	W	Ad	CH_2tBu	O*t*Bu	−2.8	−7.6	+4.8
2	W	Ad	Me_2Pyr	O*t*Bu	−6.9	−11.3	+4.4
3	W	Ad	Me_2Pyr	O*t*Bu$_{F3}$	−12.4	−11.3	−1.1
4	W	Ad	Me_2Pyr	O*t*Bu$_{F6}$	−15.2	−14.5	−0.7
5	W	Oxo	CH_2tBu	O*t*Bu	+2.4	−6.1	+8.6
6	W	Oxo	Me_2Pyr	O*t*Bu	−2.1	−10.5	+8.4
7	W	Oxo	Me_2Pyr	O*t*Bu$_{F3}$	−4.5	−9.6	+5.1
8	W	Oxo	Me_2Pyr	OtBu$_{F6}$	−14.7	−11.1	+6.4

[a]ΔG is the Gibbs energies relative to the separated methylidene complex and ethene. Δ(TBP-SP) is the difference in Gibbs free energy between **M-TBP** and **M-SP**. [b]A positive value for ΔG means that the metallacyclobutane is higher in energy than the separated reactants. [c]A positive value means that **M-SP** is preferred over **M-TBP**.

DOI: 10.1021/acs.organomet.5b00147
Organometallics 2015, 34, 1668−1680

Table 8. M06(SMD) Gibbs Energies in kcal/mol for M(NAr)(C_3H_6)(Me_2Pyr)(Y) Complexes with Y = Large O-Based Ligand[a]

entry	M	X	Y	ΔG M-TBP[b]	ΔG M-SP[b]	Δ(TBP-SP)[c]	exp
1	Mo	Me_2Pyr	ODIPP	−9.6	−8.7	−0.9	
2	Mo	Me_2Pyr	OTPP	−3.9	−5.6	+1.7	
3	Mo	Me_2Pyr	HIPTO	−1.8	+1.3	−3.1	
4	W	Me_2Pyr	ODIPP	−11.5	−18.1	+0.3	
5	W	Me_2Pyr	OTPP	−11.3	−9.3	−2.0	TBP[31]
6	W	Me_2Pyr	HIPTO	−6.1	+2.1	−8.2	

[a]ΔG is the Gibbs energy relative to the separated methylidene complex and ethene. Δ(TBP-SP) is the difference between **M-TBP** and **M-SP**. [b]A positive value for ΔG means that the metallacyclobutane is higher in energy than the separated reactants. [c]A positive value means that **M-SP** is preferred over **M-TBP**.

becomes the more favorable isomer when E is an aryl-imido group, and Y is strongly electron withdrawing or also a very bulky ligand ($OtBu_{F6}$, $OtBu_{F9}$ and HIPTO). Y ligands of moderate electron donating effect and relatively small size ($OtBu_{F3}$ and ODIPP) yield **M-TBP** and **M-SP** close in energy.

While no ligands are trans to each other in **M-SP** since the four basal ligands are not coplanar, the **M-TBP** structure has two apical trans ligands, which maximizes the trans influence. Consequently, the **M-TBP** isomer can be more stable than **M-SP** only if the two apical ligands are relatively weak donors. Since the E ligand is always at the apical site, it is better to have an aryl imido than the more electron donating alkyl imido or oxo (which behaves as a very strong donating ligand). Conversely, it is better to have a fluoroalkoxy or an aryloxy over an alkoxy, for the other apical ligand Y, the worst case being pyrrolyl and alkyl ligands. Furthermore, making Y more bulky also favors **M-TBP** as clearly evidenced in the series Y = ODIPP, OTPP, HIPTO.

M-TBP Isomerization vs Cycloreversion and Consequences for Alkene Metathesis. As already mentioned, **M-TBP** is directly on the alkene metathesis pathway, while **M-SP** is not (Scheme 1). However, **M-TBP** isomerization into the typically more stable **M-SP** structure leads to a decrease of the activity of the catalysts or even open deactivation pathways.[14,23] We thus compare the Gibbs energy barriers for the isomerization and cycloreversion processes for a large selection of systems shown in groups 1 and 2 of Scheme 2.

The transition states for the TBP-SP isomerization, TS(TBP-SP), were located using B3PW91 level of theory, and the reported energies result from single point M06 calculations at the B3PW91 geometry.[82] The calculations reveal that the geometrical features of TS(TBP-SP) are similar for all systems. Consequently, we only show the first coordination sphere around the metal for W(NAr)(C_3H_6)($OtBu_{F6}$)$_2$ in TS(TBP-SP) as an illustrative example (Figure 4). Table 9 reports the geometrical parameters of TS(TBP-SP), and Table 10 gives the corresponding computed Gibbs energy barriers relative to the

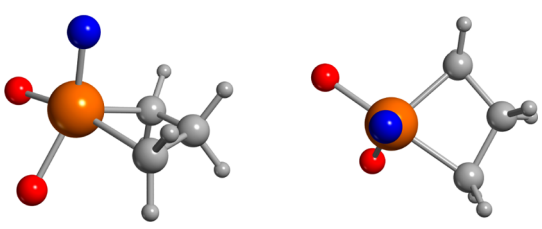

Figure 4. First coordination sphere in the TS(TBP-SP) for W(NAr)(C_3H_6)($OtBu_{F6}$)$_2$.

Table 9. Ranges in Selected Structural Parameters in TS(TBP-SP)[a]

structural parameters	ranges	
M	Mo	W
d(M-E) E = NAr	1.72−1.74	1.74−1.77
d(M-E) E = NAd	1.71−1.73	1.73−1.76
d(M-C_α)	2.10−2.16	2.13−2.17
d(M-$C_{\alpha'}$)	2.03−2.08	2.06−2.09
d(C_α-C_β)	1.56−1.58	1.56−1.58
d(M-C_β)	2.42−2.55	2.51−2.59
θ(X-M-C_α)	161−172	165−173
θ(C_α-C_β-$C_{\alpha'}$)	108−114	109−112
θ (C_α-M-$C_{\alpha'}$)	73−81	73−76
Ω(C_α-M-$C_{\alpha'}$-C_β)	6−11	9−16

[a]Distances *d* are given in Å, and angles θ and dihedral angles Ω are given in degrees.

TBP metallacyclobutane isomer ($\Delta G^{\ddagger}_{TS(TBP\text{-}SP)}$). In Table 10, we also include the energy barriers for ethene metathesis ($\Delta G^{\ddagger}_{TS(EM)}$) (metallacyclobutane to methylidene complex + ethene) relative to the TBP isomer. In addition, the histogram in Figure 5 allows for a comparison of the two processes as a function of the ligand set.[83]

The TBP-SP isomerization takes place through a turnstile process that involves the rotation of the X, Y, and E ligands relative to the two α carbons of the metallacyclobutane.[84] The structure of the transition state, which is intermediate between TBP and SP, is associated with a change in the geometrical parameters of the 4-membered ring (i.e., the M···C_β distance is between 2.5 and 2.6 Å, while the M-C_α-C_β-$C_{\alpha'}$ torsional angle is between 6 and 16°). One key feature of the transition state is that in all cases, the X ligand is almost trans to one of the metal-C_α bonds (161 to 173°), while the angle Y-M-$C_{\alpha'}$ remains far from 180° (ranging from 110° to 129°). The Gibbs free energies of the transition states for the TBP-SP isomerization (relative to the TBP isomer) range from 10.6 to 24.7 kcal/mol. Overall, the influence of the metal is typically small: the transition state for Mo is in general about 1−2 kcal/mol higher than that for W with identical ligands. The influence of the ligands, in particular X, on the energies of TS(TBP-SP) is greater; the highest transition states being for X = Me_2Pyr. Thus, the X-ligand influences strongly the energy barrier of the isomerization process, probably because it is positioned essentially trans to a M-C bond at the transition state.

The E ligand has modest influence on the energy of TS(TBP-SP) for bis-alkoxy complexes (Table 10 and Figure 5). Changing the aryl imido into an adamantyl imido ligand increases the Gibbs energy of TS(TBP-SP) by less than 2.5 kcal/mol. However, the effect is more pronounced for X =

DOI: 10.1021/acs.organomet.5b00147
Organometallics 2015, 34, 1668−1680

Table 10. M06(SMD) Gibbs Energy Barriers in kcal/mol of the TBP-SP Interconversion ($\Delta G^{\ddagger}_{TS(TBP\text{-}SP)}$) and the Ethene Metathesis Reaction ($\Delta G^{\ddagger}_{TS(EM)}$) for M(NR)($C_3H_6$)(X)(Y)

entry	M	E	X	Y	$\Delta G^{\ddagger}_{TS(TBP\text{-}SP)}$	$\Delta G^{\ddagger}_{TS(EM)}$
1	W/Mo	NAr	O*t*Bu	O*t*Bu	10.6/12.5	15.0/10.4
2	W/Mo	NAr	O*t*Bu$_{F3}$	O*t*Bu$_{F3}$	13.4/15.6	18.5/12.9
3	W/Mo	NAr	O*t*Bu$_{F6}$	O*t*Bu$_{F6}$	14.0/16.1	21.7/14.7
4	W/Mo	NAr	O*t*Bu$_{F9}$	O*t*Bu$_{F9}$	12.5/11.0	22.9/15.4
5	W/Mo	NAr	Me_2Pyr	O*t*Bu	16.7/16.7	18.8/13.4
6	W/Mo	NAr	Me_2Pyr	O*t*Bu$_{F3}$	15.7/17.9	20.3/15.7
7	W/Mo	NAr	Me_2Pyr	O*t*Bu$_{F6}$	13.7/15.7	18.9/13.1
8	W/Mo	NAr	Me_2Pyr	ODIPP	17.9/19.6	23.4/17.4
9	W/Mo	NAd	O*t*Bu	O*t*Bu	11.3/10.9	17.5/12.9
10	W/Mo	NAd	O*t*Bu$_{F3}$	O*t*Bu$_{F3}$	15.0/15.9	22.3/16.7
11	W/Mo	NAd	O*t*Bu$_{F6}$	O*t*Bu$_{F6}$	11.8/13.5	22.4/16.5
12	W/Mo	NAd	Me_2Pyr	O*t*Bu	21.1/22.1	20.3/15.5
13	W/Mo	NAd	Me_2Pyr	O*t*Bu$_{F3}$	23.3/24.7	23.0/17.8
14	W/Mo	NAd	Me_2Pyr	O*t*Bu$_{F6}$	20.7/22.4	24.6/19.0

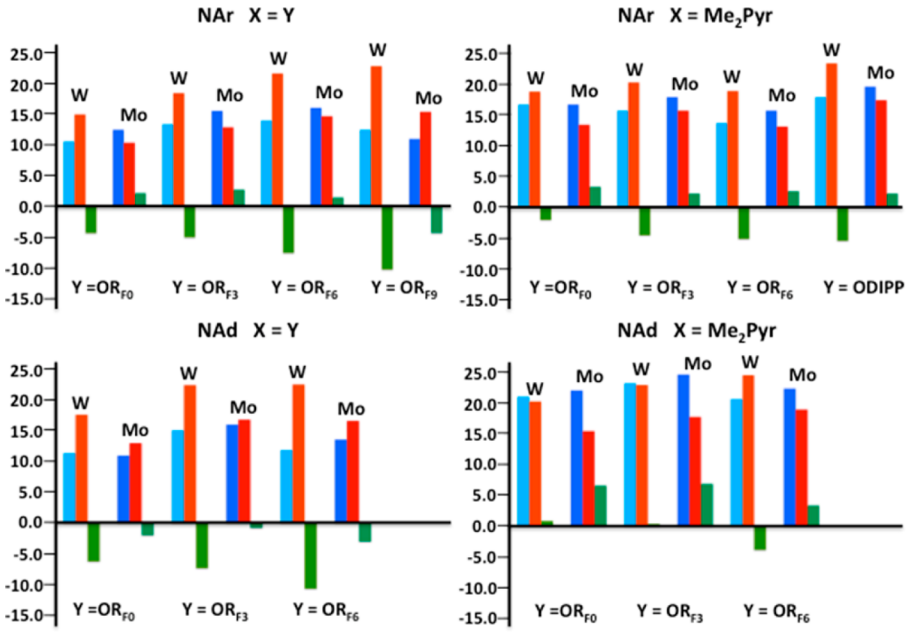

Figure 5. M06(SMD) Gibbs energy barriers in kcal/mol for the TBP-SP isomerization (light blue for W; dark blue for Mo) and ethene metathesis (orange for W; red for Mo) relative to the energy of the TBP metallacyclobutane. Differences ($\Delta\Delta G$) between the barriers of the two processes are in green. A positive value of $\Delta\Delta G$ indicates that TBP-SP isomerization is energetically more difficult than cycloreversion.

Me_2Pyr. In these cases, changing the aryl imido by the more electron donating adamantyl imido ligand raises the corresponding transition state by over 5 kcal/mol. It is unlikely to be of electronic origin, but it can be attributed to steric repulsion as illustrated in Figure 6, which shows TS(TBP-SP) for W(E)(C_3H_6)(X)(O*t*Bu$_{F6}$) (X = O*t*Bu$_{F6}$ or Me_2Pyr and E = NAr or NAd). Regardless of the nature of the E ligand, the O*t*Bu$_{F6}$ ligand extends away from the metal and remains far from the imido group. In contrast, the dimethylpyrrolyl ligand behaves differently depending on the nature of E. It forms repulsive close contacts with the adamantyl substituent of the imido ligand when E = NAd (several short H···H contacts around 2.2−2.4 Å between the methyl group of Me_2Pyr cis to the imido and the adamantyl), but these steric repulsions are not present when the imido bears a flat aryl substituent. Noteworthy, these short contacts cannot be avoided by rotation of neither the adamantyl group nor the Me_2Pyr due to the presence of the bulky O*t*Bu$_{F6}$ ligand as the Y ligand, thus showing that the adamantly imido has greater steric constraint than the aryl imido in this particular transition state.[85]

The energies of the transition states for ethene metathesis, $\Delta G^{\ddagger}_{TS(EM)}$, range from 15.0 to 24.6 for W and from 10.4 to 19.0 kcal/mol for Mo and for any given set of ligands; they are lower for Mo than for W by about 5 kcal/mol. This shows that the metal has a significant influence on the ethene metathesis energy profile, while it has little effect on TBP-SP isomerization (Figure 5). Consequently, isomerization is in general easier than metathesis for W with the exception of entries 12 and 13 in Table 10 (E = NAd, X = Me_2Pyr, Y = O*t*Bu and O*t*Bu$_{F3}$) where both processes have similar energy barriers. In contrast, for Mo complexes, the metathesis process has lower energy barriers than isomerization with four exceptions: entries 4, 9, and 11 in Table 10 (E = NAr and X = Y = O*t*Bu$_{F9}$; E = NAd and X = Y = O*t*Bu; and E = NAd and X = Y = O*t*Bu$_{F6}$, respectively) for which the metathesis process presents energy barriers that are around 2 kcal mol^{-1} lower in energy and entry

DOI: 10.1021/acs.organomet.5b00147
Organometallics 2015, 34, 1668−1680

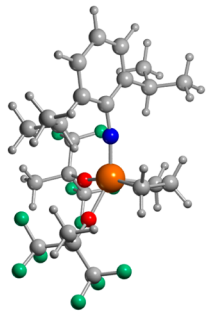

W(NAr)(C_3H_6)(O*t*Bu$_{F6}$)$_2$

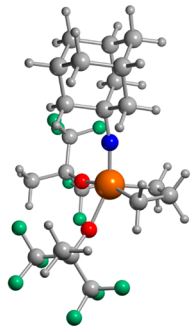

W(NAd)(C_3H_6)(O*t*Bu$_{F6}$)$_2$

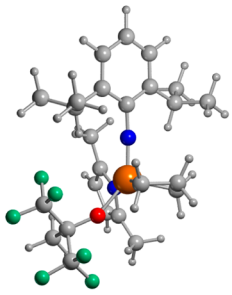

W(NAr)(C_3H_6)(Me_2Pyr)(O*t*Bu$_{F6}$)

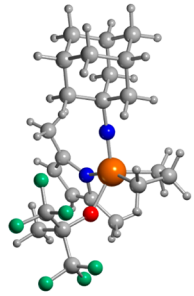

W(NAd)(C_3H_6)(Me_2Pyr)(O*t*Bu$_{F6}$)

Figure 6. TS(TBP-SP) for W(NAr)(C_3H_6)(O*t*Bu$_{F6}$)$_2$, W(NAd)-(C_3H_6)(O*t*Bu$_{F6}$)$_2$, W(NAr)(C_3H_6)(Me_2Pyr)(O*t*Bu$_{F6}$), and W(NAd)-(C_3H_6)(Me_2Pyr)(O*t*Bu$_{F6}$).

10 (E = NAd, X = Y = O*t*Bu$_{F3}$) for which the energy barriers associated with the two processes are similar.

The outcome of these calculations is that in the case of Mo, the TBP-SP isomerization is less favored than metathesis, for most ligand sets, and thus, the metallacyclobutane remains in the TBP active form. However, in the case of W, the TBP-SP isomerization competes with metathesis, hence the decrease of the concentration of **W-TBP**, when **W-SP** is more stable than **W-TBP**. As a consequence it decreases the activity of the W-catalyst in alkene metathesis by comparison with Mo.

Comparison with Experimental Systems, General Trends, and Take-Home Messages. While one should not speculate on the metallacyclobutanes that have not been characterized, it is rewarding to analyze if calculations justify the observation of those that have been isolated or characterized. Experimental and computational results agree as can be seen in Table 4 and show the following trends: (i) *W*-Metallacyclobutanes are typically much more stable than the corresponding Mo ones, consistent with the observation of several metallacyclobutanes for W and only a few for Mo. This is associated with the well-recognized stronger metal−ligand interactions for 5d compared to 4d metals. (ii) TBP structures are particularly favored with very large phenoxy Y ligand and moderate to weak donor E and X ligands (E = NAr, X = Me_2Pyr Pyr, Y = OTPP HIPTO), with bulky and strongly electron withdrawing ligands like fluoro-*t*Butyl groups (Entries (E = NAr and X = Y = O*t*BuF$_6$) and (E = NAr and X = Y = O*t*BuF$_9$)). (iii) SP structures are preferred when the catalyst contains more donating ligands, such as the E oxo ligand and/or with alkoxy X,Y groups with no fluorine. (iv) Intermediate situations, when SP and TBP isomers are observed and calculated with close relative energies, are found with intermediate electron withdrawing ligands, E = NR combined with X,Y = O*t*BuF$_3$ or ODIPP.

Remarkably for Mo, strongly electron withdrawing ligands (NAr, X = Y = O*t*BuF$_6$) stabilize the metallacyclobutane relative to the reactants (methylidene complex and ethene), allowing the isolation of a TBP isomer. Calculations confirm the stability of the metallacyclobutane relative to separated reactants but indicate a preference for SP (−9.7 kcal/mol) over TBP (−8.8 kcal/mol). However, one should note that cycloreversion and thus metathesis are associated with lower energy transition states and thereby lower energy barriers than isomerization to the more stable SP isomer (Table 10 and Figure 5). This suggests that the absence of the SP isomer could just be due to the difficulty to form this isomer in a sufficient concentration and that the increase of the efficiency of some of the catalysts, in particular Mo, could be due to the low energy barrier for metathesis combined with the difficulty to form the more stable SP isomers (high energy transition state). One such example is the Mo MAP catalyst family for which the calculations find the highest difference between the transition states for metathesis and TBP-SP isomerization (Table 9). The alternative way to have a more efficient metathesis catalyst is to increase the concentration of **M-TBP** relative to **M-SP**, which is clearly associated with the presence of an electron withdrawing ligand and/or by having at least one very large O-bearing ligand. Many highly active catalysts are of this type especially with W.

CONCLUSIONS

Metallacyclobutanes, which are intermediates in the metathesis reaction of ethene with d^0 M(E)(=CH_2)(X)(Y), have been studied with DFT (B3PW91 and M06) calculations including the solvent effect represented by a continuum SMD model, calculations with the purpose of determining and understanding their structures and energetics. The study was carried out on the "real" catalysts, namely, with the actual large ligands. They include Mo and W as metal centers, aryl, alkyl imido, and oxo ligands as E, and anionic C-, N-, and O-based ligands and in particular the very large aryloxy ligands recently described by Schrock and Hoveyda as X and Y.

Two isomeric structures are identified as minima, a trigonal bipyramidal structure **M-TBP**, and a square based pyramid **M-SP**. In both species, the α-carbon atoms of the metallacyclobutane occupy two equatorial sites and the E ligand an apical site. In **M-TBP**, the metallacyclobutane is planar with short M-C_α and long single C_α−C_β bonds, while in **M-SP**, the metallacyclobutane is folded with rather long M-C_α and normal single C_α−C_β bonds. These features are characteristic of the type of metallacyclobutane and are not significantly influenced by the metal and the ligands. As a consequence, **M-TBP** and **M-SP** have very different and characteristic ^{13}C NMR chemical shifts for the C_α and C_β atoms of the metallacyclobutane, which are very well reproduced by calculations.

The *W*-metallacyclobutanes are calculated to be always more stable relative to reactants than the *Mo*-metallacyclobutanes in good agreement with the observation of mostly tungsten metallacyclobutanes. The calculations also show a general preference for **M-SP** over **M-TBP**, this preference being in general more marked for molybdenum. **M-TBP** is the preferred isomer only when the apical ligands are weaker electron donating ligands, i.e., aryl imido > alkyl imido > oxo in combination with fluoroalkoxy or bulky aryloxy ligand > alkoxy

DOI: 10.1021/acs.organomet.5b00147
Organometallics 2015, 34, 1668−1680

ligand because it minimizes the trans influence between apical ligands. These factors influence less the **M-SP**, where no ligands are really trans to each other.

The energy barrier for TBP to SP isomerization is calculated to be lower than that for metathesis for essentially all parent *W*-metallacyclobutanes, making the SP isomer the resting state of the catalyst. In contrast, it is by and large the opposite for Mo, and the energy barrier for isomerization is typically higher than that for metathesis, making the formation of the SP isomer less favored. This is particularly true for moderately electron withdrawing X,Y ligands.

There are thus two factors that influence the efficiency of the alkene metathesis process. Since **M-TBP** is on the reaction pathway for alkene metathesis, the whole process is favored by increasing the TBP concentration and/or preventing its isomerization to the SP inactive isomer. The W catalysts for which TBP-SP isomerization is facile relative to the metathesis pathway become thus more efficient by having similar stability for the TBP and SP isomers. This is achieved by incorporating electron acceptor and/or large ligands at the apical sites. However, the Mo catalysts for which the TBP-SP isomerization is more difficult relative to the metathesis pathway can be efficient for a wider type of ligands.

These calculations, which have been performed for the parent metallacyclobutanes, provide trends that distinguish Mo and W and that highlight the specificity of X and E ligands on the behavior and roles of the metallacyclobutanes involved in alkene metathesis. We are currently exploring the effect of substituents on the overall pathways.

■ ASSOCIATED CONTENT

Supporting Information

Energetics with adamentyl imido and oxo and/or the parent pyrrolyl ligands; structural information on all calculated complexes; calculated ^{1}H and ^{13}C NMR chemical shifts; structural and energy information on all complexes. This material is available free of charge via the Internet at http://pubs.acs.org.

■ AUTHOR INFORMATION

Corresponding Authors

*(X.S.-M.) E-mail: xavi@klingon.uab.es.
*(C.C.) E-mail: ccoperet@inorg.chem.eth.ch.
*(O.E.) E-mail: odile.eisenstein@univ-montp2.fr.

Notes

The authors declare no competing financial interest.

■ ACKNOWLEDGMENTS

X.S.-M. acknowledges financial support from the MINECO (CTQ2011-24847/BQU) and the Generalitat de Catalunya (SGR2014-482). He also thanks the ETH Zürich for a visiting scientist position in 2013 and the Generalitat de Catalunya for a position of Professor Agregat Serra Húnter position. C.C. thanks ETH Zürich for financial support. O.E. thanks the CNRS and the "Ministère de l'Enseignement Supérieur et de la Recherche" for funding. This article is dedicated to the memory of Tom Ziegler.

■ REFERENCES

(1) Hérisson, J. L.; Chauvin, Y. *Makromol. Chem.* **1970**, *141*, 161−176.
(2) Chauvin, Y. *Angew. Chem., Int. Ed.* **2006**, *45*, 3740−3747.
(3) Schrock, R. R.; Hoveyda, A. H. *Angew. Chem., Int. Ed.* **2003**, *42*, 4592−4633.
(4) Schrock, R. R. *Angew. Chem., Int. Ed.* **2006**, *45*, 3748−3759.
(5) Schrock, R. R. *Chem. Rev.* **2009**, *109*, 3211−3226.
(6) Copéret, C.; Chabanas, M.; Petroff Saint-Arroman, R.; Basset, J.-M. *Angew. Chem., Int. Ed.* **2003**, *42*, 156−181.
(7) Copéret, C. *Dalton Trans.* **2007**, 5498−5504.
(8) Trnka, T. M.; Grubbs, R. H. *Acc. Chem. Res.* **2001**, *34*, 18−29.
(9) Grubbs, R. H. *Angew. Chem., Int. Ed.* **2006**, *45*, 3760−3765.
(10) Vougioukalakis, G. C.; Grubbs, R. H. *Chem. Rev.* **2010**, *110*, 1746−1787.
(11) Lwin, S.; Wachs, I. E. *ACS Catal.* **2014**, *4*, 2505−2520.
(12) Solans-Monfort, X.; Clot, E.; Copéret, C.; Eisenstein, O. *J. Am. Chem. Soc.* **2005**, *127*, 14015−14025.
(13) Poater, A.; Solans-Monfort, X.; Clot, E.; Copéret, C.; Eisenstein, O. *J. Am. Chem. Soc.* **2007**, *129*, 8207−8216.
(14) Solans-Monfort, X.; Copéret, C.; Eisenstein, O. *J. Am. Chem. Soc.* **2010**, *132*, 7750−7757.
(15) Solans-Monfort, X.; Copéret, C.; Eisenstein, O. *Organometallics* **2012**, *31*, 6812−6822.
(16) Solans-Monfort, X. *Dalton Trans.* **2014**, *43*, 4573−4586.
(17) Adlhart, C.; Chen, P. *Angew. Chem., Int. Ed.* **2002**, *41*, 4484−4487.
(18) Adlhart, C.; Chen, P. *J. Am. Chem. Soc.* **2004**, *126*, 3496−3510.
(19) Vyboishchikov, S. F.; Bühl, M.; Thiel, W. *Chem.—Eur. J.* **2002**, *8*, 3962−3975.
(20) Poater, A.; Ragone, F.; Correa, A.; Szadkowska, A.; Barbasiewicz, M.; Grela, K.; Cavallo, L. *Chem.—Eur. J.* **2010**, *16*, 14354−14364.
(21) Solans-Monfort, X.; Pleixats, R.; Sodupe, M. *Chem.—Eur. J.* **2010**, *16*, 7331−7343.
(22) Cavallo, L. *J. Am. Chem. Soc.* **2002**, *124*, 8965−8973.
(23) Leduc, A.-M.; Salameh, A.; Soulivong, D.; Chabanas, M.; Basset, J.-M.; Copéret, C.; Solans-Monfort, X.; Clot, E.; Eisenstein, O.; Böhm, V. P. W.; Röper, M. *J. Am. Chem. Soc.* **2008**, *130*, 6288−6297.
(24) Suresh, C. H.; Koga, N. *Organometallics* **2004**, *23*, 76−80.
(25) Suresh, C. H.; Baik, M.-H. *Dalton Trans.* **2005**, 2982−2984.
(26) Schrock, R. R.; DePue, R. T.; Feldman, J.; Schaverien, C. J.; Dewan, J. C.; Liu, A. H. *J. Am. Chem. Soc.* **1988**, *110*, 1423−1435.
(27) Feldman, J.; Davis, W. M.; Schrock, R. R.; Murdzek, J. S. *Organometallics* **1989**, *8*, 2266−2268.
(28) Feldman, J.; Davis, W. M.; Thomas, J. K.; Schrock, R. R. *Organometallics* **1990**, *9*, 2535−2548.
(29) Schrock, R. R.; Murdzek, J. S.; Bazan, G. C.; Robbins, J.; DiMare, M.; O'Regan, M. *J. Am. Chem. Soc.* **1990**, *112*, 3875−3886.
(30) Blanc, F.; Berthoud, R.; Copéret, C.; Lesage, A.; Emsley, L.; Singh, R.; Kreickmann, T.; Schrock, R. R. *Proc. Natl. Acad. Sci. U.S.A.* **2008**, *105*, 12123−12127.
(31) Jiang, A. J.; Simpson, J. H.; Müller, P.; Schrock, R. R. *J. Am. Chem. Soc.* **2009**, *131*, 7770−7780.
(32) Flook, M. M.; Jiang, A. J.; Schrock, R. R.; Müller, P.; Hoveyda, A. H. *J. Am. Chem. Soc.* **2009**, *131*, 7962−7963.
(33) Schrock, R. R.; Jiang, A. J.; Marinescu, S. C.; Simpson, J. H.; Möller, P. *Organometallics* **2010**, *29*, 5241−5251.
(34) Peryshkov, D. V.; Schrock, R. R.; Takase, M. K.; Müller, P.; Hoveyda, A. H. *J. Am. Chem. Soc.* **2011**, *133*, 20754−20757.
(35) Peryshkov, D. V.; Schrock, R. R. *Organometallics* **2012**, *31*, 7278−7286.
(36) Mougel, V.; Copéret, C. *Chem. Sci.* **2014**, *5*, 2475−2481.
(37) Reithofer, M. R.; Dobereiner, G. E.; Schrock, R. R.; Müller, P. *Organometallics* **2013**, *32*, 2489−2492.
(38) Feldman, J.; Schrock, R. R. *Prog. Inorg. Chem.* **1991**, *39*, 1−74.
(39) Rappé, A. K.; Goddard, W. A., III *J. Am. Chem. Soc.* **1982**, *104*, 448−456.
(40) Folga, E.; Ziegler, T. *Organometallics* **1993**, *12*, 325−331.
(41) Wu, Y.; Peng, Z. *J. Am. Chem. Soc.* **1997**, *7863*, 8043−8049.
(42) Handzlik, J. *J. Catal.* **2003**, *220*, 23−34.
(43) Goumans, T. P. M.; Ehlers, A. W.; Lammertsma, K. *Organometallics* **2005**, *24*, 3200−3206.

DOI: 10.1021/acs.organomet.5b00147
Organometallics 2015, 34, 1668−1680

(44) Handzlik, J. *J. Phys. Chem. B* **2005**, *109*, 20794−20804.
(45) Handzlik, J.; Sautet, P. *J. Catal.* **2008**, *256*, 1−14.
(46) Vasiliu, M.; Li, S.; Arduengo, A. J.; Dixon, D. A. *J. Phys. Chem. C* **2011**, *115*, 12106−12120.
(47) Schinzel, S.; Chermette, H.; Copéret, C.; Basset, J.-M. *J. Am. Chem. Soc.* **2008**, 7984−7987.
(48) Wang, C.; Haeffner, F.; Schrock, R. R.; Hoveyda, A. H. *Angew. Chem., Int. Ed.* **2013**, *52*, 1939−1943.
(49) Beer, S.; Hrib, C. G.; Jones, P. G.; Brandhorst, K.; Grunenberg, J.; Tamm, M. *Angew. Chem., Int. Ed.* **2007**, *46*, 8890−8894.
(50) Beer, S.; Brandhorst, K.; Hrib, C. G.; Wu, X.; Haberlag, B.; Grunenberg, J.; Jones, P. G.; Tamm, M. *Organometallics* **2009**, *28*, 1534−1545.
(51) Suresh, C. H.; Frenking, G. *Organometallics* **2010**, *29*, 4766−4769.
(52) Suresh, C. H.; Frenking, G. *Organometallics* **2012**, *31*, 7171−7180.
(53) Becke, A. D. *J. Chem. Phys.* **1993**, *98*, 5648−5652.
(54) Perdew, J. P.; Wang, Y. *Phys. Rev. B* **1992**, *45*, 13244−13249.
(55) Zhao, Y.; Truhlar, D. G. *Theor. Chem. Acc.* **2007**, *120*, 215−241.
(56) Andrae, D.; Häusserman, U.; Dolg, M.; Stoll, H.; Preuss, H. *Theor. Chim. Acta* **1990**, *77*, 123−141.
(57) Küchle, W.; Dolg, M.; Stoll, H.; Preuss, H. *Mol. Phys.* **1991**, *74*, 1245−1263.
(58) Ehlers, A. W.; Böhme, M.; Dapprich, S.; Gobbi, A.; Höllwarth, A.; Jonas, V.; Köhler, K. F.; Stegmann, R.; Veldkamp, A.; Frenking, G. *Chem. Phys. Lett.* **1993**, *208*, 111−114.
(59) Höllwarth, A.; Böhme, M.; Dapprich, S.; Ehlers, A. W.; Gobbi, A.; Jonas, V.; Köhler, K. F.; Stegmann, R.; Veldkamp, A.; Frenking, G. *Chem. Phys. Lett.* **1993**, *208*, 237−240.
(60) (a) Hehre, W. J.; Ditchfield, R.; Pople, J. A. *J. Chem. Phys.* **1972**, *56*, 2257−2261. (b) Hariharan, P. C.; Pople, J. A. *Theor. Chim. Acta* **1973**, *28*, 213−222.
(61) Marenich, A. V.; Cramer, C. J.; Truhlar, D. G. *J. Phys. Chem. B* **2009**, *113*, 6378−6396.
(62) Frisch, M. J.; Trucks, G. W.; Schlegel, H. B.; Scuseria, G. E.; Robb, M. A.; Cheeseman, J. R.; Scalmani, G.; Barone, V.; Mennucci, B.; Petersson, G. A.; Nakatsuji, H.; Caricato, M.; Li, X.; Hratchian, H. P.; Izmaylov, A. F.; Bloino, J.; Zheng, G.; Sonnenberg, J. L.; Hada, M.; Ehara, M.; Toyota, K.; Fukuda, R.; Hasegawa, J.; Ishida, M.; Nakajima, T.; Honda, Y.; Kitao, O.; Nakai, H.; Vreven, T.; Montgomery, J. A., Jr.; Peralta, J. E.; Ogliaro, F.; Bearpark, M.; Heyd, J. J.; Brothers, E.; Kudin, K. N.; Staroverov, V. N.; Kobayashi, R.; Normand, J.; Raghavachari, K.; Rendell, A.; Burant, J. C.; Iyengar, S. S.; Tomasi, J.; Cossi, M.; Rega, N.; Millam, J. M.; Klene, M.; Knox, J. E.; Cross, J. B.; Bakken, V.; Adamo, C.; Jaramillo, J.; Gomperts, R.; Stratmann, R. E.; Yazyev, O.; Austin, A. J.; Cammi, R.; Pomelli, C.; Ochterski, J. W.; Martin, R. L.; Morokuma, K.; Zakrzewski, V. G.; Voth, G. A.; Salvador, P.; Dannenberg, J. J.; Dapprich, S.; Daniels, A. D.; Farkas, Ö.; Foresman, J. B.; Ortiz, J. V.; Cioslowski, J.; Fox, D. J. *Gaussian 09*, revision D.01; Gaussian, Inc.: Wallingford, CT, 2009.
(63) Lee, A. M.; Handy, N. C.; Colwell, S. M. *J. Chem. Phys.* **1995**, *103*, 10095−10109.
(64) Kutzelnigg, W.; Fleischer, U.; Schindler, M. *NMR Basic Principles and Progress*; Springer-Verlag: New York, 1990; pp 165−262.
(65) Solans-Monfort, X.; Eisenstein, O. *Polyhedron* **2006**, *25*, 339−348.
(66) Blanc, F.; Basset, J.-M.; Copéret, C.; Sinha, A.; Tonzetich, Z. J.; Schrock, R. R.; Solans-Monfort, X.; Clot, E.; Eisenstein, O.; Lesage, A.; Emsley, L. *J. Am. Chem. Soc.* **2008**, *130*, 5886−5900.
(67) Paredes-Gil, K.; Solans-Monfort, X.; Rodriguez-Santiago, L.; Sodupe, M.; Jaque, P. *Organometallics* **2014**, *33*, 6065−6075.
(68) Reed, A. E.; Curtiss, L. A.; Weinhold, F. *Chem. Rev.* **1988**, *88*, 899−926.
(69) Bader, R. F. W. *Chem. Rev.* **1991**, *91*, 893−928.
(70) Since this analysis is done only on a qualitative basis, there is no need to be concerned by the charges of the two fragments.
(71) An AIM analysis carried out for the metallacyclobutane identifies the same critical points for the two isomers (two M-C_α and two C_α-C_β bond critical point and one ring critical point).
(72) The calculations of the chemical shifts do not include the spin−orbit corrections that could be important in particular for W since we are only interested in trends.
(73) Autschbach, J.; Zheng, S. *Annu. Rep. NMR Spectrosc.* **2009**, *67*, 1−95.
(74) Hrobárik, P.; Hrobáriková, V.; Meier, F.; Repiský, M.; Komorovský, S.; Kaupp, M. *J. Phys. Chem. A* **2011**, *115*, 5654−5659.
(75) Poblador-Bahamonde, A. I.; Poteau, R.; Raynaud, C.; Eisenstein, O. *Dalton Trans.* **2011**, *40*, 11321−11326.
(76) Wodyński, A.; Gryff-Keller, A.; Pecul, M. *J. Chem. Theory Comput.* **2013**, *9*, 1909−1917.
(77) Test calculations on all species presented in Table 4 show that M06 energies on B3PW91 geometries (M06//B3PW91) give results very close to those obtained optimizing with M06 (M06//M06). This result is expected from the similarities in the geometrical parameters.
(78) Conley, M. P.; Mougel, V.; Peryshkov, D. V.; Forrest, W. P.; Gajan, D.; Lesage, A.; Emsley, L.; Copéret, C.; Schrock, R. R. *J. Am. Chem. Soc.* **2013**, *135*, 19068−19070.
(79) (a) Forrest, W. P.; Weis, J. G.; John, J. M.; Axtell, J. C.; Simpson, J. H.; Swager, T. M.; Schrock, R. R. *J. Am. Chem. Soc.* **2014**, *136*, 10910−10913. (b) Mougel, V.; Pucino, M.; Copéret, C. *Organometallics* **2015**, *34*, 551−554.
(80) Conley, M. P.; Forrest, W. P.; Mougel, V.; Copéret, C.; Schrock, R. R. *Angew. Chem., Int. Ed.* **2014**, *53*, 14221−14224.
(81) Townsend, E. M.; Hyvl, J.; Forrest, W. P.; Schrock, R. R.; Müller, P.; Hoveyda, A. H. *Organometallics* **2014**, *33*, 5334−5341.
(82) This approach is validated by the strong similarities in the structures obtained from the B3PW91 and M06 calculations as shown in Table 1.
(83) It should be mentioned that the transition state located for this process is similar to that previously assigned to the alkene coordination step and that all attempts to locate a transition state associated with the cycloreversion of the metallacyclobutane failed.
(84) Ugi, I.; Marquarding, D.; Klusacek, H.; Gillespie, P.; Ramirez, F. *Acc. Chem. Res.* **1971**, *4*, 288−296.
(85) Ibrahem, I.; Yu, M.; Schrock, R. R.; Hoveyda, A. H. *J. Am. Chem. Soc.* **2009**, *131*, 3844−3845.

DOI: 10.1021/acs.organomet.5b00147
Organometallics 2015, 34, 1668−1680